CHIN. PHYS. LETT. Vol. 35, No. 4 (2018) 040401

Phase Transition and Quasinormal Modes for Spherical Black Holes in 5D Gauss–Bonnet Gravity *

Ming Zhang(张明)[1,2**], Rui-Hong Yue(岳瑞宏)[3**]

[1]*Faculty of Science, Xi'an Aeronautical University, Xi'an 710077*

[2]*National Joint Engineering Research Center of Special Pump System Technology, Xi'an 710077*

[3]*Center for Gravitation and Cosmology, College of Physical Science and Technology, Yangzhou University, Yangzhou 225009*

(Received 28 November 2017)

We study the quasinormal modes (QNMs) of massless scalar perturbations to probe the van der Waals like SBH/LBH phase transition of anti-de Sitter black holes in five-dimensional (5D) Gauss–Bonnet gravity. It is found that the signature of this SBH/LBH phase transition is detected when the slopes of the QNMs frequency change drastically and differently in small and large black holes near the critical point. The obtained results further support that the QNMs can be a dynamic probe to investigate the thermodynamic properties in black holes.

PACS: 04.50.Kd, 04.70.−s, 04.25.D− DOI: 10.1088/0256-307X/35/4/040401

The thermodynamical phase transition of a black hole is always a hot topic in the black hole physics community. A great deal of attention has been paid to studying the phase transition of black holes in anti-de Sitter (AdS) space mainly due to the AdS/CFT correspondence.[1−3] Recently thermodynamics of AdS black holes has been generalized to the extended phase space where the cosmological constant is treated as the pressure of the black hole,[4] and it was found that a first order small black hole and large black hole phase transition is allowed, which is superficially analogous to a liquid-gas phase transition of the van der Waals fluid. More discussions in this direction can be found as well, including reentrant phase transitions and more general van der Waals behavior.[5−22]

For a long time, black hole thermodynamical phase transitions are supposed to be detected by some observational signatures. When considering the quasinormal modes (QNMs) of dynamical perturbations, which are characteristic sounds of black holes, it is expected that the black hole phase transitions can be reflected in the dynamical perturbations in their surrounding geometries through frequencies and damping times of the oscillations. In AdS black holes, thermodynamic phase transition in the dual field theory corresponds to the onset of instability of a black hole, therefore it is naturally considered that QNMs of black holes have some connections with thermodynamic phase transitions of strongly coupled field theories.[23] With numerous investigations on this issue, researchers have found more and more evidence between thermodynamical phase transitions and dynamical perturbations.[24−34]

In addition, following the advent of string theory, extra dimensions were promoted from an interesting curiosity to a theoretical necessity since superstring theory requires an eleven-dimensional spacetime to be consistent from a quantum point of view.[35−38] Among the higher curvature gravities, the most extensively studied theory is the so-called Gauss–Bonnet gravity,[39−46] which naturally emerges when we generalize Einstein's theory in higher dimensions by keeping all characteristics of usual general relativity excepting the linear dependence of the Riemann tensor. Until now, this van der Waals-like SBH/LBH phase transition for a spherical horizon black hole was also recovered in the Gauss–Bonnet gravity.[47−51] Motivated by these results, in this work, we study whether the signature of van der Waals like SBH/LBH phase transition of AdS black holes with correction of the Gauss–Bonnet term can be reflected by the dynamical QNMs behavior in the massless scalar perturbation. The dynamical perturbations in the isobaric process will be discussed in the context of the van der Waals phase transition picture.

The action of five-dimensional (5D) Gauss–Bonnet gravity in the cosmological constant Λ can be written as

$$\mathcal{I} = \frac{1}{16\pi}\int d^5x\sqrt{-g}[-2\Lambda + R + \alpha(R_{\gamma\delta\lambda\sigma}R^{\gamma\delta\lambda\sigma} - 4R_{\gamma\delta}R^{\gamma\delta} + R^2)], \quad (1)$$

where α is the Gauss–Bonnet coefficient with dimension (length)^2, and is positive in the heterotic string theory.

The solution of the 5D GB-AdS black hole is[49]

$$ds^2 = -f(r)dt^2 + \frac{1}{f(r)}dr^2 + r^2 d\Omega_3^2, \quad (2)$$

$$f(r) = 1 + \frac{r^2}{2\tilde{\alpha}}\left(1 - \sqrt{1 - \frac{16\pi\tilde{\alpha}P}{3} + \frac{32\tilde{\alpha}M}{3\pi r^4}}\right), \quad (3)$$

*Supported by the National Natural Science Foundation of China under Grant Nos 11647050, 11675139 and 51575420, and the Scientific Research Program Funded by Shaanxi Provincial Education Department under Grant No 16JK1394.

**Corresponding author. Email: zhangming@xaau.edu.cn; rhyue@yzu.edu.cn

© 2018 Chinese Physical Society and IOP Publishing Ltd

where M is the black hole mass. In the extended phase space, the cosmological constant Λ is regarded as a variable and also identified with the thermodynamic pressure $P = -\frac{\Lambda}{8\pi}$ in the geometric units $G_{\rm N} = \hbar = c = k = 1$. We will only consider the positive GB coefficient $\tilde{\alpha} = 8\pi G_{\rm N}\alpha$ in the following. If we take $\tilde{\alpha} \to 0$, the solution $f(r)$ reduces to the SAdS case. To have a well-defined vacuum solution with $M = 0$, the Gauss–Bonnet coefficient $\tilde{\alpha}$ and the pressure P have to satisfy the following constraint $0 < \frac{16\pi\tilde{\alpha}P}{3} \leq 1$.

In terms of the horizon radius r_+, the mass M, the Hawking temperature T and entropy S of GB-AdS black holes can be written as[49]

$$M = \frac{3\pi r_+^2}{8} + \frac{3\pi\tilde{\alpha}}{8} + \frac{\pi^2 P r_+^4}{2}, \tag{4}$$

$$T = \frac{(8\pi P r_+^2 + 3)r_+}{6\pi(r_+^2 + 2\tilde{\alpha})}, \ S = \frac{\pi^2 r_+^3}{2}\Big(1 + \frac{6\tilde{\alpha}}{r_+^2}\Big). \tag{5}$$

In the extended phase space, the black hole mass M is considered as the enthalpy H rather than the internal energy of the gravitational system.

From the Hawking temperature Eq. (4), we can obtain the equation of state as follows:

$$P = \frac{3}{4r_+}\Big(1 + \frac{2\tilde{\alpha}}{r_+^2}\Big)T - \frac{3}{8\pi r_+^2}. \tag{6}$$

As usual, a critical point occurs when P has an inflection point

$$\frac{\partial P}{\partial r_+}\Big|_{T=T_{\rm c}, r_+=r_{\rm c}} = \frac{\partial^2 P}{\partial r_+^2}\Big|_{T=T_{\rm c}, r_+=r_{\rm c}} = 0. \tag{7}$$

Then we can obtain the corresponding critical values

$$r_{\rm c} = \sqrt{6\tilde{\alpha}}, \ T_{\rm c} = \frac{1}{2\pi\sqrt{6\tilde{\alpha}}}, \ P_{\rm c} = \frac{1}{48\pi\tilde{\alpha}}. \tag{8}$$

The behavior of the Gibbs free energy G is important to determine the thermodynamic phase transition. The free energy G obeys the following thermodynamic relation $G = H - TS$ with

$$G = \frac{1}{24(r_+^2 + 2\tilde{\alpha})}[3\pi(r_+^4 - 3\tilde{\alpha}r_+^2 + 6\tilde{\alpha}^2) - 4\pi^2 r_+^4(r_+^2 + 18\tilde{\alpha})P], \tag{9}$$

where r_+ is understood as functions of pressure and temperature, $r_+ = r_+(P, T)$, via the equation of state, i.e., Eq. (6).

Following Refs. [4,48,49], we can define three dimensionless parameters

$$p = \frac{P}{P_{\rm c}}, \ t = \frac{T}{T_{\rm c}}, \ \gamma = \frac{r_+}{r_{\rm c}}. \tag{10}$$

Therefore, we can obtain the dimensionless form of Eq. (6)

$$p = \frac{3}{\gamma}\Big(1 + \frac{1}{3\gamma^2}\Big)t - \frac{3}{\gamma^2}. \tag{11}$$

The p–γ isotherm diagram is shown in Fig. 1. The dotted line corresponds to the 'idea gas' phase behavior when $T > T_{\rm c}$, and the van der Waals like small-large black hole phase transition appears in the system when $T < T_{\rm c}$.

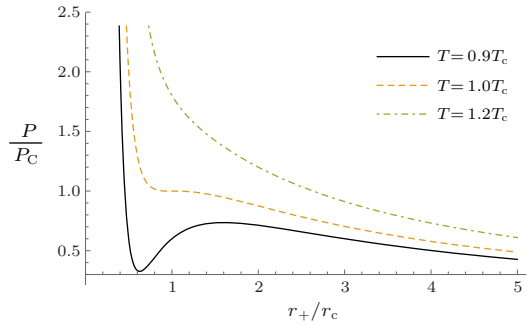

Fig. 1. The p–γ diagram.

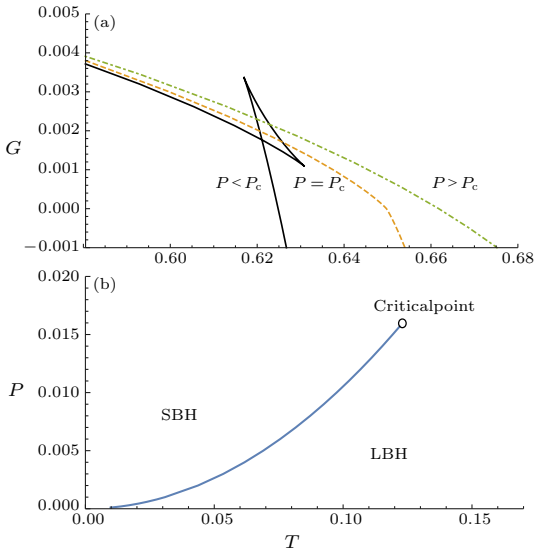

Fig. 2. The Gibbs free energy G (upper panel) and coexistence line of small-large black holes phase transition (lower panel).

In upper panel of Fig. 2, we can see that the G surface demonstrates the characteristic 'swallow tail' behavior, which shows that there is a van der Waals like first order phase transition in the system. The lower panel of Fig. 2 shows the coexistence line in the P–T plane by finding a curve where the Gibbs free energy and temperature coincide for small and large black holes. The coexistence line is very similar to that in the van der Waals fluid. The critical point is shown by a small circle at the end of the coexistence line. The small-large black hole phase transition occurs for $T < T_{\rm c}$.

For a van der Waals liquid-gas system, the liquid-gas structure does not change suddenly but undergoes the second order phase transition at the critical point ($V = V_{\rm c}$, $T = T_{\rm c}$, $P = P_{\rm c}$). This is described by Ehrenfest's description.[52,53] In conventional thermodynamics, Ehrenfest's description consists of the first

and second Ehrenfest's equations[54,55]

$$\frac{\partial P}{\partial T}\Big|_S = \frac{C_{P2}-C_{P1}}{TV(\zeta_2-\zeta_1)} = \frac{\Delta C_P}{TV\Delta\zeta}, \tag{12}$$

$$\frac{\partial P}{\partial T}\Big|_V = \frac{\zeta_2-\zeta_1}{\kappa_{T2}-\kappa_{T1}} = \frac{\Delta\zeta}{\Delta\kappa_T}. \tag{13}$$

For a genuine second order phase transition, both of these equations have to be satisfied simultaneously. Here ζ and κ_T denote the volume expansion and isothermal compressibility coefficients of the system, respectively,

$$\zeta = \frac{1}{V}\frac{\partial V}{\partial T}\Big|_P, \quad \kappa_T = -\frac{1}{V}\frac{\partial V}{\partial P}\Big|_T. \tag{14}$$

Using a similar method to the one used in Ref. [48], we can find that this phase transition at the critical point in the 5D GB-AdS black hole is of the second order (Ehrenfest's equation is satisfied in this case). This result is consistent with the nature of the liquid-gas phase transition at the critical point.

Now we study the evolution of a massless scalar field perturbation in the surrounding geometry of the 5D GB-AdS black hole.

The radial part of the perturbation, $\Phi(r,t) = \phi(r)e^{-i\omega t}$, is described by the Klein–Gordon equation

$$\frac{1}{\sqrt{-g}}\partial_\mu(\sqrt{-g}g^{\mu\nu}\partial_\nu\Phi(r,t)) = 0. \tag{15}$$

Then the radial function $\phi(r)$ obeys the following differential equation

$$\phi''(r) + \Big(\frac{f'(r)}{f(r)} + \frac{2}{r}\Big)\phi'(r) + \frac{\omega^2\phi(r)}{f(r)^2} = 0, \tag{16}$$

where ω is a complex number $\omega = \omega_{\rm r} + i\omega_{\rm im}$, corresponding to the QNM frequencies of the oscillations describing the perturbation. The imaginary part $\omega_{\rm im}$ must be negative since the QNMs decay in time.

Here we define $\phi(r)$ as $\varphi(r)\exp[-i\int\frac{\omega}{f(r)}dr]$, where $\exp[-i\int\frac{\omega}{f(r)}dr]$ asymptotically approaches to the ingoing wave near horizon, then Eq. (16) becomes

$$\varphi''(r) + \varphi'(r)\Big(\frac{f'(r)}{f(r)} - \frac{2i\omega}{f(r)} + \frac{2}{r}\Big) - \frac{2i\omega}{rf(r)}\varphi(r) = 0. \tag{17}$$

For Eq. (17), we have $\varphi(r) = 1$ in the limit of $r \to r_+$. At the AdS boundary ($r \to \infty$), we need $\varphi(r) = 0$. Under these boundary conditions, we can numerically solve Eq. (17) to find QNM frequencies by adopting the shooting method.

Fixing the pressure P, we can plot the T–r_+ diagram of GB-AdS black holes in the upper panel of Fig. 3. For $P < P_{\rm c}$, there is an inflection point and the behavior is reminiscent of the van der Waals system. The critical point can be obtained from

$$\frac{\partial T}{\partial r_+}\Big|_{P=P_{\rm c},r_+=r_{\rm c}} = \frac{\partial^2 T}{\partial r_+^2}\Big|_{P=P_{\rm c},r_+=r_{\rm c}} = 0. \tag{18}$$

The behavior of the Gibbs free energy is plotted in the lower panel of Fig. 3. The cross point 5 between the solid line marked as 1–5 and the solid line denoted as 4–5 shows that the Gibbs free energy and P coincide for small and large black holes. In the upper panel of Fig. 3, point 5 is separated into L5 and R5 for the same Gibbs free energy and the chosen $T_* \approx 0.4479$ where the small and large black holes can coexist. Moreover, the physical phase marked between points 1–5 or 1–L5 is for the small black hole, while the physical phase indicated between points 5–4 or R5–4 is for the large black hole.

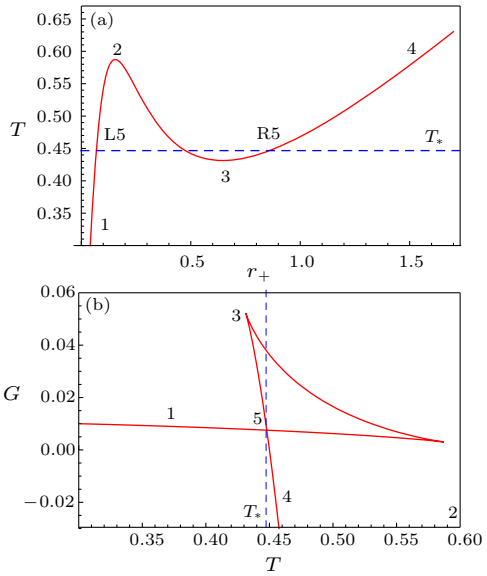

Fig. 3. The T–r_+ (upper panel) and G–T (lower panel) diagrams for $\tilde{\alpha} = 0.01$ and $P = 0.2387$.

In Table 1, we further list the QNM frequencies of massless scalar perturbation around small and large black holes for first order SBH/LBH phase transition. With regard to the small black hole phase, the radius of a black hole becomes smaller and smaller when the temperature decreases from phase transition temperature T_*. In this process the absolute values of the imaginary part of QNM frequencies decrease, while the real part frequencies change slightly. On the other hand, when the temperature for large black hole phase increases from the phase transition temperature T_*, the black hole becomes larger. The QNM frequencies increase in both the real part and the absolute value of the imaginary part. This means that the massless scalar perturbation outside the black hole has more oscillations but it decays faster. These results are consistent with the overall discussions reported in Refs. [33,34]. Figure 4 illustrates the QNM frequencies for small and large black hole phases. The increase of the black hole's size is indicated by the arrows.

In addition, at the critical position $P = P_{\rm c}$, with $P_{\rm c} \simeq 0.663146$, a second-order phase transition occurs. The QNM frequencies of the small and large black hole phases are plotted in Fig. 5. We can see that QNM frequencies of the two black hole phases

possess the same behavior as the black hole horizon increases at the critical point.

Table 1. The QNM frequencies of massless scalar perturbation with the change of the black hole temperature. The upper part, above the horizontal line, is for the small black hole phase, while the lower part is for the large black hole phase.

T	r_+	ω
0.444	0.068101	$3.90534 - 0.022251i$
0.445	0.068341	$3.90509 - 0.022399i$
0.446	0.068581	$3.90483 - 0.022548i$
0.447	0.068822	$3.90457 - 0.022698i$
0.4475	0.068944	$3.90444 - 0.022774i$
0.448	0.86978	$4.34349 - 2.25505i$
0.4485	0.87356	$4.35069 - 2.26628i$
0.449	0.87730	$4.35784 - 2.27739i$
0.450	0.88465	$4.37198 - 2.29924i$
0.451	0.89185	$4.38593 - 2.32065i$

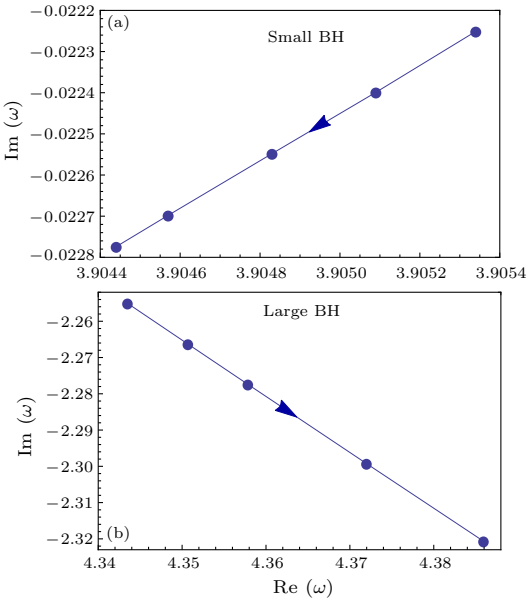

Fig. 4. The behavior of QNMs for large and small black holes in the complex-ω. The arrow indicates the increase of the black hole horizon.

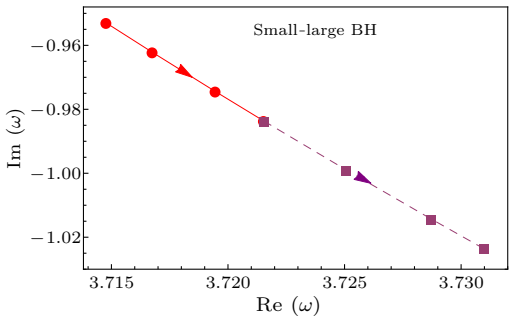

Fig. 5. The behavior of QNM frequencies for large (dashed) and small (solid) black holes in the complex-ω. The arrow indicates the increase of the black hole horizon.

In summary, we have calculated the QNMs of massless scalar perturbations around small and large 5D AdS black holes in the Gauss–Bonnet gravity. When the van der Waals analogy SBH/LBH phase transition appears in the extended space, the slopes of the QNM frequency change drastically and differently in the small and large black hole phases as the horizon radius r_+ increases. This clearly presents the signature of the phase transition between small and large black holes. Moreover, we have also found that, at the critical isobaric phase transitions, QNM frequencies for both small and large black holes have the same behavior, suggesting that QNMs are not appropriate to probe the black hole phase transition in the second order.

This is one more example showing that the QNM can provide dynamical physical phenomenon of the thermodynamic phase transition. Since the QNM is expected to be detected and there is strong astrophysical interest, its ability to reflect the thermodynamic phase transition is interesting, which is expected to disclose the observational signature of the thermodynamic phase transition.

References

[1] Maldacena J 1999 *Int. J. Theor. Phys.* **38** 1113
Maldacena J 1998 *Adv. Theor. Math. Phys.* **2** 231
[2] Gubser S S, Klebanov I R and Polyakov A M 1998 *Phys. Lett.* B **428** 105
[3] Witten E 1998 *Adv. Theor. Math. Phys.* **2** 253
[4] Kubiznak D and Mann R B 2012 *J. High Energy Phys.* **1207** 033
[5] Gunasekaran S, Mann R B and Kubiznak D 2012 *J. High Energy Phys.* **1211** 110
[6] Hendi S H and Vahidinia M H 2013 *Phys. Rev.* D **88** 084045
[7] Zhao R, Zhao H H, Ma M S and Zhang L C 2013 *Eur. Phys. J.* C **73** 2645
[8] Zou D C, Zhang S J and Wang B 2014 *Phys. Rev.* D **89** 044002
[9] Dehghani M H, Kamrani S and Sheykhi A 2014 *Phys. Rev.* D **90** 104020
[10] Hennigar R A, Brenna W G and Mann R B 2015 *J. High Energy Phys.* **1507** 077
[11] Zhang L C, Ma M S, Zhao H H and Zhao R 2014 *Eur. Phys. J.* C **74** 3052
[12] Altamirano N, Kubiznak D, Mann R B and Sherkatghanad Z 2014 *Galaxies* **2** 89
[13] Wei S W and Liu Y X 2015 *Phys. Rev. Lett.* **115** 111302
Wei S W and Liu Y X 2016 *Phys. Rev. Lett.* **116** 169903
[14] Xu W and Zhao L 2014 *Phys. Lett.* B **736** 214
[15] Sadeghi J, Pourhassan B and Rostami M 2016 *Phys. Rev.* D **94** 064006
[16] Hansen D, Kubiznak D and Mann R B 2017 *J. High Energy Phys.* **1701** 047
[17] Zeng X X and Li L F 2016 *Adv. High Energy Phys.* **2016** 6153435
[18] Hendi S H, Panah E B, Panahiyan S and Talezadeh M S 2017 *Eur. Phys. J.* C **77** 133
[19] Xu J, Cao L M and Hu Y P 2015 *Phys. Rev.* D **91** 124033
[20] Zou D C, Yue R H and Zhang M 2017 *Eur. Phys. J.* C **77** 256
[21] Hendi S H, Mann R B, Panahiyan S and Panah E B 2017 *Phys. Rev.* D **95** 021501
[22] Rajagopal A, Kubizňák D and Mann R B 2014 *Phys. Lett.* B **737** 277
[23] Gubser S S and Mitra I 2001 *J. High Energy Phys.* **0108** 018
[24] Mahapatra S 2016 *J. High Energy Phys.* **1604** 142
[25] Rao X P, Wang B and Yang G H 2007 *Phys. Lett.* B **649** 472
[26] He X, Wang B, Cai R G and Lin C Y 2010 *Phys. Lett.* B **688** 230

[27] Berti E and Cardoso V 2008 *Phys. Rev.* D **77** 087501
[28] Shen J, Wang B, Lin C Y, Cai R G and Su R K 2007 *J. High Energy Phys.* **0707** 037
[29] Koutsoumbas G, Musiri S, Papantonopoulos E and Siopsis G 2006 *J. High Energy Phys.* **0610** 006
[30] Zou D C, Liu Y, Zhang C Y and Wang B 2016 *Europhys. Lett.* **116** 40005
[31] Zou D C, Liu Y and Yue R H 2017 *Eur. Phys. J.* C **77** 365
[32] Zangeneh M K, Wang B, Sheykhi A and Tang Z Y 2017 *Phys. Lett.* B **771** 257
[33] Liu Y, Zou D C and Wang B 2014 *J. High Energy Phys.* **1409** 179
[34] Chabab M, El Moumni H, Iraoui S and Masmar K 2016 *Eur. Phys. J.* C **76** 676
[35] Horava P and Witten E 1996 *Nucl. Phys.* B **475** 94
[36] Lukas A, Ovrut B A and Waldram D 1999 *Phys. Rev.* D **60** 086001
[37] Randall L and Sundrum R 1999 *Phys. Rev. Lett.* **83** 3370
[38] Randall L and Sundrum R 1999 *Phys. Rev. Lett.* **83** 4690
[39] Lanczos C 1938 *Ann. Math.* **39** 842
[40] Lovelock D 1971 *J. Math. Phys.* **12** 498
[41] Zou D C, Yang Z Y, Yue R H and Yu T Y 2011 *Chin. Phys.* B **20** 100403
[42] Yue R H, Zou D C, Yu T Y and Yang Z Y 2011 *Chin. Phys.* B **20** 050401
[43] Zhou K, Yang Z Y, Zou D C and Yue R H 2012 *Chin. Phys.* B **21** 020401
[44] Boulware D G and Deser S 1985 *Phys. Rev. Lett.* **55** 2656
[45] Izumi K 2014 *Phys. Rev.* D **90** 044037
[46] Wheeler J T 1986 *Nucl. Phys.* B **273** 732
[47] Xu W, Xu H and Zhao L 2014 *Eur. Phys. J.* C **74** 2970
[48] Zou D C, Liu Y and Wang B 2014 *Phys. Rev.* D **90** 044063
[49] Cai R G, Cao L M, Li L and Yang R Q 2013 *J. High Energy Phys.* **1309** 005
[50] Wei S W and Liu Y X 2014 *Phys. Rev.* D **90** 044057
[51] He S, Li L F and Zeng X X 2017 *Nucl. Phys.* B **915** 243
[52] Bruno L 1983 *Thermodynamics and Introductory Statistical Mechanics* (New York: Wiley Online Library) p 119
[53] Stanley H E 1987 *Introduction to Phase Transitions and Critical Phenomena* (Oxford: Oxford University Press)
[54] Nieuwenhuizen T M 1997 *Phys. Rev. Lett.* **79** 1317
[55] Zemansky M W and Dittman R H 1997 *Heat and Thermodynamics: an Intermediate Textbook* (New York: McGraw-Hill)